Indian Journal of Radio & Space Physics
Vol. 38, October 2009, pp. 260-265

Some studies of solar flare effects on the propagation of sferics and a transmitted signal

B K De[1], S S De[2,*], B Bandyopadhyay[2], Suman Paul[2], S Barui[2] & D K Haldar[2]

[1]Department of Physics, Tripura University, Tripura (West), Suryamaninagar 799 130, India
[2]Centre of Advanced Study in Radio Physics and Electronics, University of Calcutta, Kolkata 700 009, India
*Email: de_syam_sundar@yahoo.co.in

Received 19 May 2009; revised received and accepted 15 September 2009

Apart from diurnal and seasonal variations, integrated field intensity of sferics (IFIS) exhibits characteristic variations in relation to various geophysical and solar events like geomagnetic storms, meteor showers, solar X-ray flares and solar radio emission. Continuous monitoring of IFIS at frequencies 1, 3, 6, 9 and 12 kHz from Agartala (latitude 23ºN) are being made over the last several years. The analyses of some preliminary observations in relation to solar flares are reported in the paper. Solar flare effects on the propagation of transmitted signals at 16.3 kHz recorded in Kolkata (latitude 22.56ºN) during November 2004 have also been presented.

Keywords: Ionosphere, Geomagnetic storms, Solar flare, Sunspots, Sferics

PACS Nos.: 94.20.*wg*; 94.20.Vv; 96.60.*qe*

1 Introduction

The electromagnetic radiations from cloud discharges are known as atmospherics or sferics. The Fourier spectrum extends from extremely low frequency (ELF) to high frequency (HF). The contribution is mostly from very low frequency (VLF) band. During severe thunderstorms, contribution to the radiation field from ELF band is also remarkable. An important characteristic of thundercloud is the consistent polarity of their cloud-to-ground lightning flashes. The majority of flashes bring negative charge to the surface of the Earth.

The atmospherics are very much significant in regard to electric phenomenon going on in different types of cloud during meteorologically active periods. During clear period, atmospheric radio noise field strength (ARNFS), i.e. IFIS measurement provides different aspects of ionospheric propagation. Tripura, in the North-East part of India, is the privileged place to study ARNFS from the local cloud discharge as well as from the distant sources of Australia, Japan and Africa.

The interest in ELF-VLF atmospherics is due to the following reasons: (i) ELF-VLF spectrum between 50 Hz and 10 kHz is unusual since there is no broadcast transmitter in this range; (ii) as long as the receiver is operated well away from unwanted short range electromagnetic interference, the spectrum is dominated largely by natural noise from cloud discharge; (iii) work on propagation in relation to solar disturbances, earthquakes, meteor showers and geomagnetic study of ELF-VLF atmospherics in North-East part of India is scanty; (iv) the characteristics of ELF-VLF sferics in relation to solar activity are still to be explored in this region. In this paper, the outcome of some studies have been reported on the effects of solar flares on sferics at different frequencies recorded at Tripura and also on the transmitted signals (VTX1) at 16.3 kHz from a navy station in India, recorded in Kolkata, on 23 November 2004.

Flares release energy in the form of electromagnetic radiation and through the energetic particles (electrons and protons). All flares have high emissions in the wavelength range 1–8 Å. The intense radiations from solar flares when travel towards the Earth, enhancement of D-region ionization occurs[1-4]. Solar flares cause significant perturbations in the received ELF-VLF sferics and VLF signals propagating in the Earth-ionosphere waveguide over a long distance[5].

Stratospheric electric fields get modified due to conductivity enhancements caused by the energetic particles during solar flares[6]. Several works have been

reported earlier on statistical relationship between the occurrences of solar flares and variations of lower atmospheric electricity parameters[7,8].

2 Experiment

The integrated field intensity of sferics has been recorded using narrow band receivers at 1, 3, 6, 9 and 12 kHz. By proper selection of bands, the unwanted noises have been reduced. The filter output is amplified with AC amplifier. The AC amplifier is constructed using high slew-rate OP AMP in the non-inverting mode. The AC amplifier is followed by series resonant circuit tuned at the desired frequency and another buffer. The selective circuit consisted of a series combination of an inductance and a capacitance. To ensure high selectivity, the inductive coil has been mounted inside a pot-core of ferrite material. The voltage induced across the inductive element is Q-factor times the output of AC amplifier.

The selected sinusoidal Fourier component atmospherics is then applied to the input of a detector circuit through a unit gain buffer. The detector circuit has been constructed using a diode in the negative rectifying mode. The output of the diode is applied across parallel combination of R and C so that the detecting time constant is 0.22 s. The level of detected envelope is proportional to the amplitude of the Fourier component. The output is calibrated with respect to input using standard signal generator followed by attenuator of 0.2 dB resolution. At Kolkata, continuous recording of different VLF sferics and transmitted signals is being continued.

The experimental set-up for VLF recording consists of an inverted L-type antenna made from 8 SWG copper wire of 120 m length to receive vertically polarized atmospherics in the VLF bands from near and far sources. It has been installed horizontally at a height of about 30 m above the ground. The signal processor is used to tune the desired frequencies. The overall Q-factor of the tuning circuit is around 300. The signals from the tuning stage are fed to a log amplifier. The data are recorded by digital data acquisition system card.

Specific features of 16.3 kHz sub-ionospheric signals

Location of transmitter: Vijayananarayanam, India

Latitude: 8.43ºN

Longitude: 77.8ºE

Transmitting antenna: Omni-directional

Power of radiation: 4 kW with continuous operation.

X-ray flare data have been taken from NOAA GOES12 satellite. X-ray flux in the wavelength ranges 0.5-4 Å and 1-8 Å are recorded by GOES satellite. X-ray flux are classified into three groups: (i) X-ray flares having short duration termed as spikes (SPIKY); (ii) X-ray flares having rise time smaller than one-fourth the duration termed as impulsive (IMP); and (iii) X-ray flares with both rise time and decay time greater than one-fourth the duration known as gradual rise and fall type flares (GRF).

Sudden enhancement in sferics (SES) and sudden enhancement in signal amplitude (SESA)

During solar flare, the level of sferics enhances within several minutes, which is known as sudden enhancement in sferics (SES). The amplitude of VLF signal from a transmitting station also enhances. This is termed as sudden enhancement in signal amplitude (SESA). Both events follow the sequences of enhanced solar radiation. To study the effect of solar position on SES, each year has been divided into four solar phases:

P1: The Sun moves from Tropic of Cancer to Equator (21 June-21 September)

P2: The Sun moves from Equator to Tropic of Capricorn (22 September-21 December)

P3: The Sun moves from Tropic of Capricorn to Equator (22 December-21 March)

P4: The Sun moves from Equator to Tropic of Cancer (22 March-21 June)

3 Observations and analyses

In the absence of local cloud activity, sferics are characterized by sunrise (SR) and sunset (SS) effects. It is seen that diurnal pattern reveals higher levels at night and at afternoon hours. During sunrise period, the level of atmospherics decreases gradually to remarkably low value. During afternoon, the level increases. During sunset, the level again decays slightly showing a minimum which is called sunset minimum. This diurnal pattern is highly affected by local thunderstorm and cloud activities.

ELF-VLF sferics exhibit fall in level during the sunrise period. In general, this kind of fall is obtained in meteorologically clear days. The fall is characterized by 2 or 3 small steps. The magnitude of total fall lies between 8-15 dB. It may be mentioned that during overhead shower and geomagnetically active days (A_p>50), the sunrise effect disappears. The ELF-VLF sferics exhibit gradual fall followed by gradual rise during sunset. This is termed as sunset effect.

The sferics exhibit zig-zag variation during rainy days (Fig.1). The diurnal character is lost. The sunrise effect and sunset effect are merged in the zig-zag variations. Figure 2 shows records of X-ray flares and sudden enhancement in sferics (SES) (900 Hz considered as 1 kHz). Figure 3 depicts SES at 9 kHz on 31 August 2004. SES on two successive days, 21and 22 July 2004, are presented in Fig. 4.

The commencement time of SES slightly lags behind that of X-ray flares. A similar time difference is also observed between the peaks of SES and X-ray flares. Period of data is from January 2003 to December 2004. Number of SES observed is 671. The detail of the percentage association of SES with solar X-ray flares at different frequencies and solar phases are presented in Table 1. At all frequencies and in all the three types of flares, percentage correlation decreases from phase P1 to P4. In all the phases, percentage correlation is highest for GRF type of flares and least in the case of SPIKY forms in all the solar phases. The percentage correlation with respect to variation of frequency is highest at 9 kHz and least at 12 kHz.

There is always a time lag between the commencement of X-ray flare and the commencement of SES. The variations of delay time with respect to different types of flares are estimated and shown in Fig. 5. The delay time is highest for GRF type flares and least for SPIKY flares. The delay time with respect to variation of solar phase is least in P1 and highest in P3.

The depth of the phenomenon may be expressed in terms of enhancement in sferics per unit increase in flux (SES per unit increase in solar flux) and has been shown in Fig. 6. In all the cases, the depth is highest in the case of IMPULSIVE flares. At 1, 3 and 12 kHz sferics, depth is smallest for SPIKY flares, whereas at 6 and 9 kHz, depth is least in the case of GRF type of flares.

Fig. 7 shows sudden enhancement in signal amplitude (SESA) at 16.3 kHz associated with solar flare at X-rays of 1-8 Å. The morphological structure of the variation of signal amplitude is similar to the evolution of solar X-ray flare. The percentage association of SESA has been shown in Table 2. It decreases in going from phase P1 to P2. In all solar phases, the percentage association is highest in the case of IMPULSIVE type X-ray flares.

The variation of delay time between the SESA and X-ray flares with solar phases for the three types of flares are exhibited in Fig. 8. The delay time for GRF type flares is maximum in P2 phase, while it is maximum in P3 phase in case of IMPULSIVE and SPIKY type flares.

4 Discussion

The dominant process of electron production in the quiescent D-region is the photo-ionization of nitric oxide by H_α-radiation. Galactic cosmic radiation is also partially responsible for ionization in D-region. Although contribution of the solar X-radiation to the

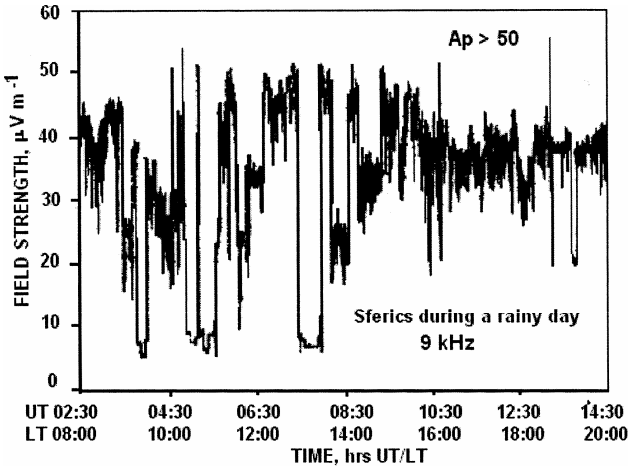

Fig. 1 — Sferics at 9 kHz during a rainy day at Tripura

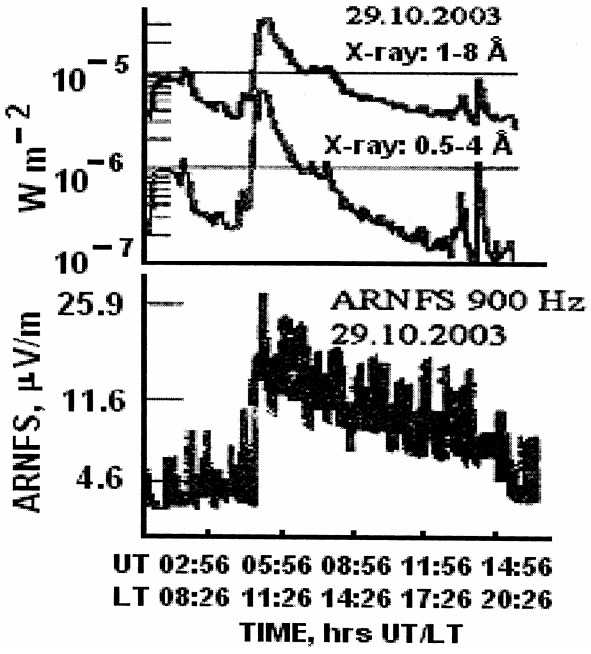

Fig. 2 —X-ray flares and associated sudden enhancement in sferics (SES) at 900 Hz on 29 October 2003. The abscissa shows time in UT /LT and the ordinate shows X-ray flux at wavelength bands 0.1-0.8 nm and 0.05-0.4 nm in W m^{-2} and level of atmospherics in terms RMS field strength μV/m

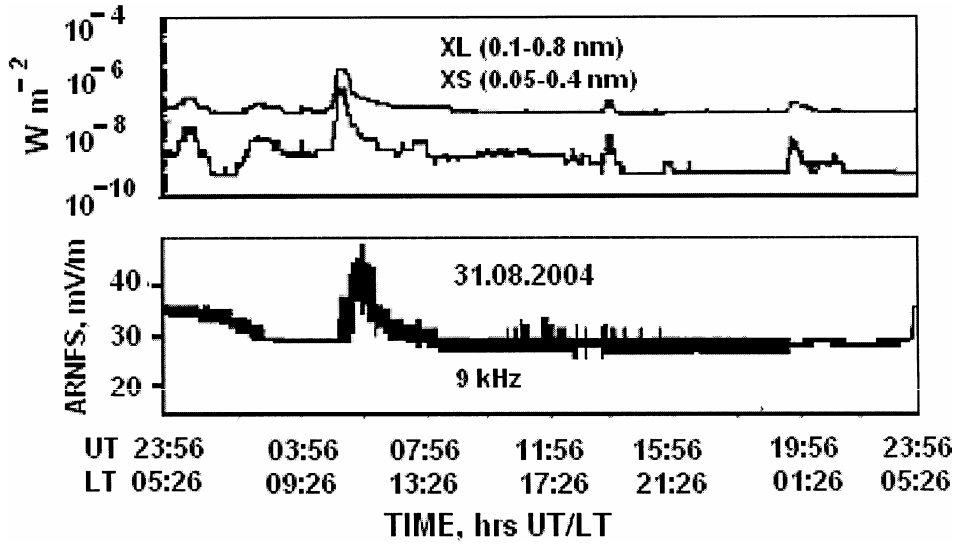

Fig. 3 —SES at 9 kHz on 31 August 2004 associated with X-ray flux enhancement. The level of atmospherics is in terms of induced voltage at the antenna

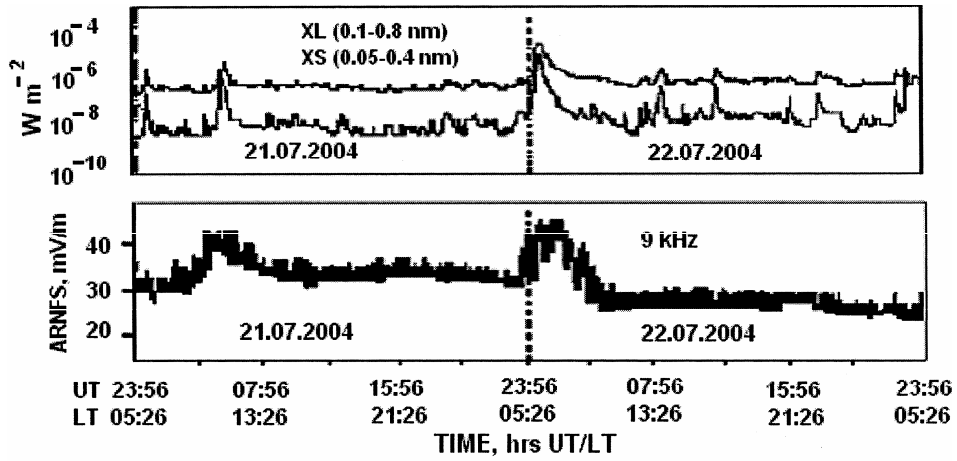

Fig. 4 —SES at 9 kHz on two successive dates 21 and 22 July 2004 associated with X-ray flux enhancement

Table 1 — Details of the percentage association of SES with solar X-ray flares at various frequencies and solar phases

Frequency, kHz	Phase	IMPULSIVE	GRF	SPIKY
1 and 3	P1	61	65	55
	P2	58	61	52
	P3	52	58	48
	P4	48	55	46
6	P1	68	71	61
	P2	64	67	57
	P3	56	62	53
	P4	52	59	48
9	P1	72	76	64
	P2	68	71	61
	P3	62	66	58
	P4	57	61	52
12	P1	67	72	62
	P2	62	65	58
	P3	55	62	53
	P4	52	60	49

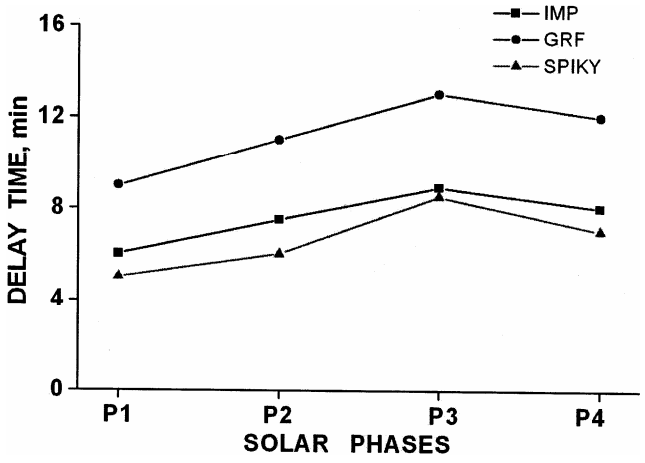

Fig. 5 — Variations of average delay time of three different types of flares with solar phases

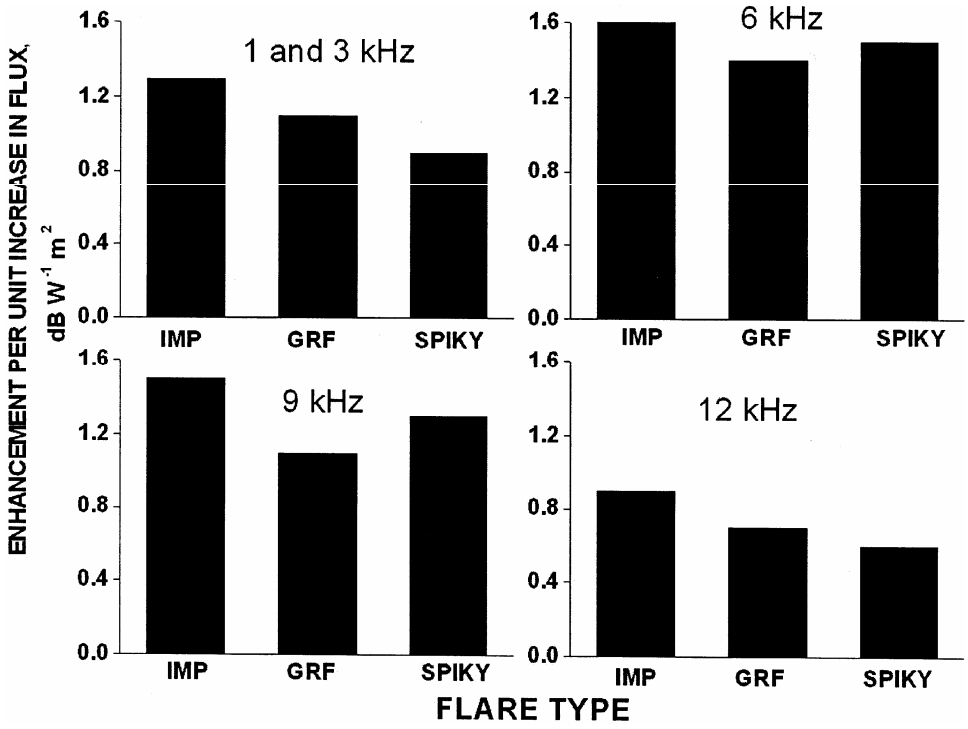

Fig. 6 — Variation in the magnitude of enhancement of sferics for three different types of flares with solar phases

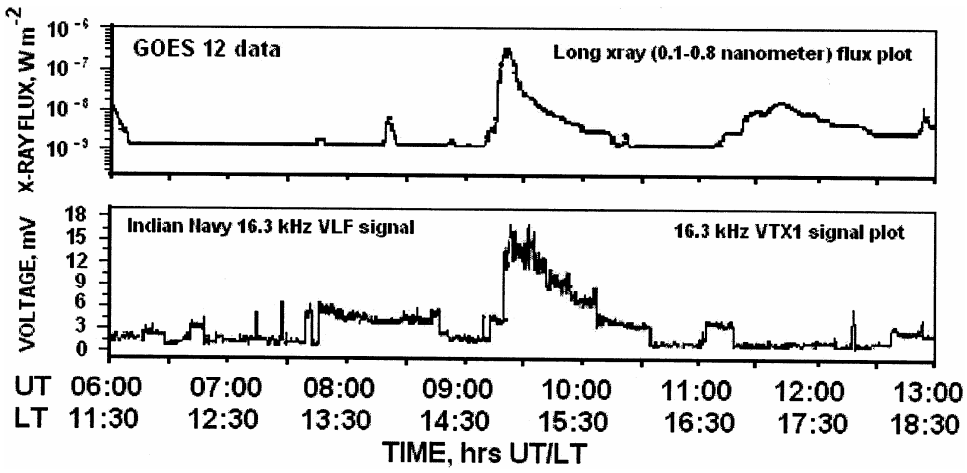

Fig. 7 —Sudden enhancement in signal amplitude (SESA) during a solar flare on 23 November 2004

formation of D-region is small, solar X-radiation <10 Å is mostly responsible for extra-ionization during solar flare condition[4, 9].

Normal electron density of the D-region is $(3 \times 10^7) - (6 \times 10^7)$ m^{-3}. During X-ray flare, D-region electron density increases by 7–35 times[3]. As a result, conductivity parameter of the D-region increases and reflection height of ELF-VLF radio wave decreases. These give rise to better propagation condition.

It may be noted (as an example) that the normal reflection height of 40 kHz signal is 70 km. The normal electron density near 65 km is in the range $(30 \times 10^6) - (60 \times 10^6)$ m^{-3}. During an X-ray flare, the electron density increases by about 7 to 35 times the normal value. An increase of about 85 times at an altitude of 70 km may occur. The electron density near 65 km usually increased between (150×10^6) and (950×10^6) m^{-3}. In this situation, the 40 kHz signal is expected to be reflected from about 65 km. There are two competing processes caused by a flare-related increase in electron density, viz.: (i) a decrease in the height of the earth-ionosphere waveguide (responsible

Table 2 — Percentage association of SESA with the three different types of X-ray flares

Frequency, kHz	Phase	IMPULSIVE	GRF	SPIKY
16.3	P1	62	65	58
	P2	56	59	52
	P3	47	53	43
	P4	42	46	49

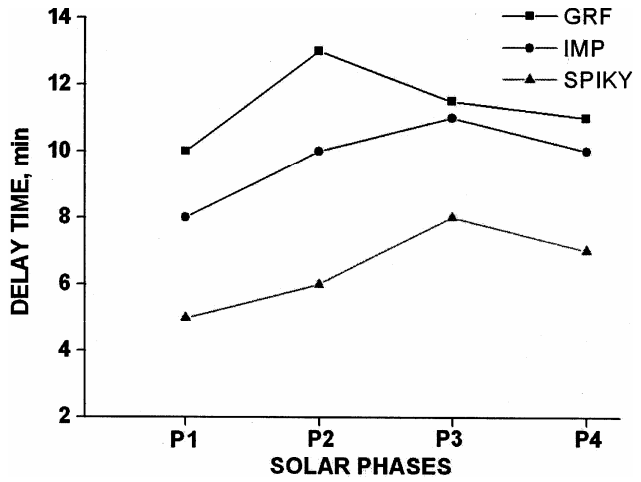

Fig. 8 — Variations of delay time between SESA and X-ray flares with solar phases for the three different types of flares

for SDA); and (ii) an increase in the conductivity of the upper boundary of the waveguide due to a steeper electron density gradient, which allows better reflection, i.e. lower absorption is responsible for SES. As regard to the wavelength, the former factor does not play a role and one therefore, observes SES. After the commencement of solar X-ray flare, it requires certain time for the ionization level to reach to an optimum value to give better situation for wave-guide mode of propagation[5]. This is dependent on the rate of extra-ionization during flare. This is the reason for time delay of SES with respect to solar X-ray flare. The depth of enhancement depends upon the phase difference between first and second modes which are comparable during extra-ionization[10]. Thus X-ray flares undoubtedly produce extra ionization at an altitude of 65 – 70 km but the characteristics of the sudden enhancement of signal strength at 40 kHz over a long distance east-west propagation path are not only dependent on this extra ionization and recombination, but also on climatic conditions such as temperature, humidity and their product.

5 Conclusions

In the light of the above results, it is concluded that:

1 In all the solar phases, the percentage association of SES is highest at 9 kHz and lowest at 1-3 kHz.
2 At all the frequencies, percentage association is highest for GRF type flares.
3 Delay time is lowest for SPIKY flares and highest for GRF flares.
4 Magnitude of enhancement is highest at 6 kHz.
5 For constant frequency, amount of enhancement is highest for IMPULSIVE type of flares.

Acknowledgement

The authors gratefully acknowledge the financial support provided by Indian Space Research Organization (ISRO) through S K Mitra Centre for Research in Space Environment, University of Calcutta, Kolkata, India.

References

1 Muraoka Y, Murata H & Sato T, The quantitative relationship between VLF phase deviations and 1 - 8 Å solar X-ray fluxes during solar flares, *J Atmos Terr Phys (UK)*, 39 (1977) 787.
2 Mechtly E A, Bowhill S A & Smith L G, Changes of lower ionosphere electron concentrations with solar activity, *J Atmos Terr Phys (UK)*, 34 (1972) 1899.
3 Thomson N R & Clilverd M A, Solar flare induced ionospheric D-region enhancements from VLF amplitude observations, *J Atmos Sol-Terr Phys (UK)*, 63 (2001) 1729.
4 McRae W M & Thomson N R, Solar flare induced ionospheric D-region enhancements from VLF phase and amplitude observations, *J Atmos Sol-Terr Phys (UK)*, 66 (2004) 77.
5 Mitra A P, *Ionospheric effects of solar flares* (D Reidel, Dordrecht-Holland/ Boston-USA), 1974.
6 Holtzworth R H & Mozer F S, Direct evidence of solar flare modification of stratospheric electric fields, *J Geophys Res (USA)*, 84 (1979) 363.
7 Cobb W E, Evidence of solar influence on the atmospheric electric elements at Mauna Loa Observatory, *Mon Weather Rev (USA)*, 95 (1967) 905.
8 Reiter R, Further evidence of impact of solar flares on potential gradient and air-earth current characteristics at high mountain stations, *Pure App Geophys (Switzerland)*, 86 (1971) 142.
9 Pacini A A & Raulin J P, Solar X-ray flares and ionospheric sudden phase anomalies relationship: A solar cycle phase dependence, *J Geophys Res (USA)*, 111 (2006) A09301, doi: 1029/2006JA011613.
10 Lynn K J W, VLF mode conversion observed at mid-latitude, *J Atmos Terr Phys (UK)*, 35 (1973) 439.